

Performance analysis of modified dynamic voltage restorer (DVR) employed to a grid connected solar PV system

Rakeshwri Pal^{1*}, Sushma Gupta¹

¹ MANIT, Bhopal

*Corresponding author E-mail: rakeshwri.pal19@gmail.com

Abstract

Among various power quality problems, voltage sag and swell are dominant where loads are very sensitive to the voltage disturbances. Various custom power devices are introduced recently to overcome these voltage issues, dynamic voltage restorer (DVR) is one of them. It offers very cost effective solution for problems such as voltage sag, swell and harmonics by establishing the proper voltage level during voltage disturbances to protect sensitive loads. In this paper, performance of DVR to improve power quality is done for solar photovoltaic (PV) based generation system feeding the grid and the three phase linear load. Solar PV generation system is implemented with an incremental conductance (IC) maximum power point tracking (MPPT) technique. The DVR is connected in between solar PV system and load. The basic structure of DVR is modified by using the photovoltaic system as an alternative to DC source and in place of conventional 2-level voltage source converter (VSC) neutral point clamped (NPC) multi level inverter is used. The system performance is analyzed in the MATLAB/Simulink environment. The simulation results justified the efficiency of modified DVR in the mitigation of voltage sag in distribution system. Improvement of power quality by stabilizing voltage during fault and promoting renewable energy is the main framework of this work.

Keywords: Custom Power Device; Dynamic Voltage Restorer; Multilevel Inverter; Maximum Power Point Tracking (MPPT); Solar PV.

1. Introduction

Power quality problems such as sags, swells, transients, interruptions and harmonics directly affect the electric load. Among these sag appeared as a most severe power quality problem. It can cause improper functioning and eventual tripping of industrial equipments, leading to the production loss and revenue [1]. According to the IEEE 519-1992 and IEEE 1159-1195 standards sag is decrease to between 0.1 and 0.9 pu in rms voltage or current at the power frequency for durations from 0.5 cycle to 1 min. Dynamic Voltage Restorer (DVR) is a Custom Power Device (CPD) used to mitigate voltage sags/swells and to normalize load voltage. This device economically achieves the protection of sensitive loads from distortions, supply voltage unbalance and voltage sags/swells, it improves power quality by providing the voltage compensation, also it has additional features such as reactive power compensation and harmonic compensation [2]. In conventional DVR topology, its power circuit consists of an injection transformer, a harmonic filter, an energy storage device/DC voltage source, a voltage source inverter (VSI) and a bypass switch [3]. The structure of DVR includes a DC voltage source that can provide the active power. The active power compensation capability of the DVR depends on the capacity of the energy storage device/DC voltage source and the employed compensation technique [4-5]. Due to recent trends towards the renewable energy sources, the solar photovoltaic (PV) system proposed as an alternative DC voltage source in this paper as it does not produce noise, harmful emission or polluting gases and it is fuel free. A modular solar PV system can be quickly installed anywhere, also there is no mechanical parts to wear out or break down and requires minimum maintenance to keep the system running. The electric power produced by the solar PV system can

be considered economically viable. The DVR without solar PV system supported by battery, super capacitor and fuel cell as energy storage device/DC voltage source for power quality improvement in electrical distribution system is presented in Ref. [6-8]. Solar PV supported DVR with DC-DC boost converters are incorporated to function as a high capacity DC voltage source presented in Ref. [9] and in order to attain the optimal utilization of solar PV system, a simple DC-DC converter associated through a function called MPPT technique is presented in Ref. [10] for single phase distribution system. Solar PV generation system and small hydro turbine generation system connected to the grid and DVR are presented in Ref. [11-12] and the research work with solar PV supported DVR have been carried out with PI controller presented in Ref. [9-11]. To mitigate voltage sag DVR with PI controller provides the most effective solution by establishing the proper voltage level [13-15]. Through this, it has been found that power quality investigation has been ample scope for three phase DVR supported by solar PV system under faulted conditions. The scope of work presented in this paper is to offer a model based analytical approach to design a solar PV supported DVR, where IC MPPT technique extracts maximum power from solar PV generation system and DVR with space vector control schemes are used in three phase DVR system, and highlighted with simulation results.

2. Modeling of DVR system

In this section modeling of proposed DVR system is presented along with its control and compensation technique. In the proposed DVR conventional 2-level, inverter is replaced with the multilevel inverter to reduce harmonics and solar PV array is used in place of energy storage device/DC voltage source.

2.1. DVR system design

DVR is connected in series with the distribution system to protect the electrical load which is highly sensitive to the voltage disturbances. In this proposed system DVR is connected with solar PV based generation system as shown in figure 1. The main components of a DVR are the control unit, DC voltage source, injection transformer, a harmonic filter and Voltage source converter (VSC). In the proposed DVR design, a PV system is added in to function like a DC voltage source and a five level neutral point clamped (NPC) multilevel inverter (MLI) as a VSC and the output of VSC is controlled by PI controller.

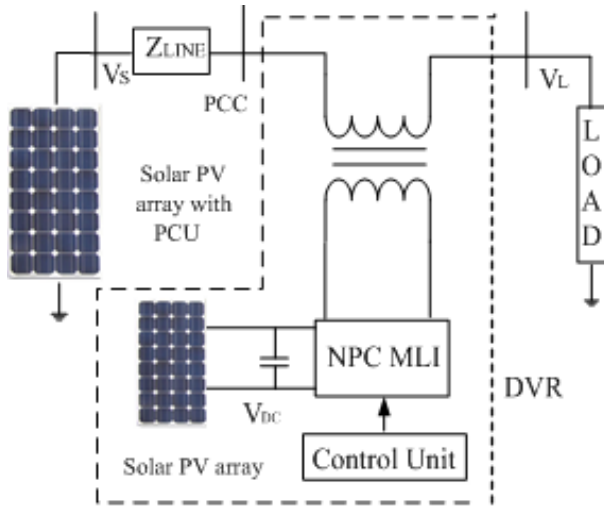


Fig. 1: Proposed DVR System

2.2. DVR modelling

The general design of the DVR consists of power circuit and control circuit. Equivalent circuit as shown in figure 2 and equation is as under

$$V_{DVR} = V_L + Z_{TH} I_L + V_{TH} \tag{1}$$

Where V_L is desired load voltage magnitude, Z_{TH} is load impedance, I_L is load current and V_{TH} is system voltage (during faulty condition).

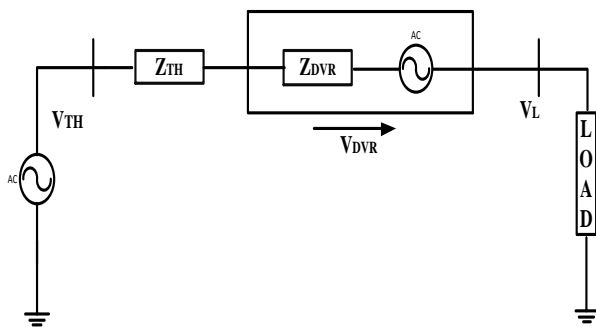


Fig. 2: Equivalent Circuit of DVR.

The load current I_L is given by:

$$I_L = \frac{P_L + jQ_L}{V_L} \tag{2}$$

When V_L is considered as a reference equation can be written as:

$$V_{DVR} \angle \alpha = V_L \angle 0 + Z_{TH} I_L \angle (\beta - \theta) + V_{TH} \angle \delta \tag{3}$$

Where α is angle of V_{DVR} , β is angle of Z_{TH} , δ is angle of V_{TH} and θ is load power angle.

$$\theta = \tan^{-1} \frac{Q_L}{P_L} \tag{4}$$

The complex power injection of the DVR can be mathematically given by:

$$S_{DVR} = V_{DVR} I_L^* \tag{5}$$

2.3. Neutral point clamped (NPC) multilevel inverter

Figure 3 shows a block diagram of a solar PV fed three-phase 5-level NPC in star configuration, this converter generates a 5-level of DC voltage which is provided by the solar PV array in DVR section using the switching function algorithm. The advantages of multi level inverter as compared to conventional 2-level inverter are when the number of output level increases harmonics of the output voltage, current as well as electromagnetic interference (EMI) decreases and also reduces switching stresses on devices [16-18]. The basic concept of a multilevel inverter is to achieve high power, high voltage by using power semiconductor switches in series with several small rating dc voltage sources to perform the conversion of power by generating a staircase voltage waveform with low total harmonic distortion (THD). The NPC structure of MLI makes the entire system flexible in terms of power capability and very simple to implement. The solar PV modeling adopted for solar PV supported DVR will be discussed in section 3.2.

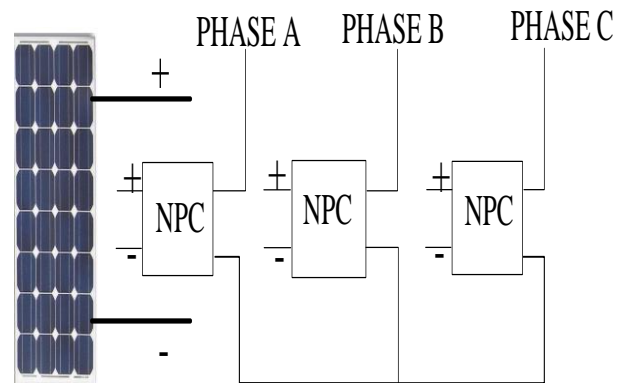


Fig. 3: Block Diagram of a Solar PV Fed 3-Φ, 5-Level NPC in Star Configuration.

2.4. Control of DVR system

In the DVR section, the control scheme as shown in figure 4 is used to maintain a constant voltage magnitude at the load terminal under voltage disturbance. In this controller, a 3- ϕ discrete phase locked loop (PLL) is used in order to track the angular frequency and phase shift of 3- ϕ voltage. The basic purpose of a controller used in a DVR is the finding of sag events in the load voltage; computation of the required voltage for compensation, and then generation of gating pulses for VSC accordingly. The dqo conversion or Park's transformation is utilized to run the operation of DVR. This method provides the information about sag deepness and phase shift along with its start and end time. The voltage parameters are expressed in the form of instantaneous space vectors. In this voltage is firstly converted from a-b-c reference frame to d-q-o reference. For ease zero sequence components is not taken into account. Figure 4 demonstrates a flow chart of dqo transformation for sags detection in load voltage. The detection is brought out for voltage of each phase among three. The control idea for the this proposed system is based on the difference between voltage reference and the measured load voltage (V_a, V_b, V_c). The voltage sags is observed as the supply voltage falls below 90% of the reference. The resulting error (difference) signal is utilized as a modulation signal that permits the gating pulses for the voltage source inverter. The gating pluses are generated through the sinusoidal pulse width modulation (SPWM) system. The injected voltages are controlled via the modulation. The phase locked loop (PLL) is employed to produce a unit sinusoidal

signal in phase with reference voltage. The generated signal is employed as switching pulses for NPC MLI. The role of SPWM is to compare a sinusoidal signal (V_{ref}) of 50 Hz frequency with a triangular signal ($V_{carrier}$) of 5 kHz to generate the pulses. When the control (sinusoidal) signal is more than the carrier (triangular) signal, the switches are ON, and their counter switches are OFF at the same time. The output voltage provided by NPC MLI mitigates the voltage sag [12-14].

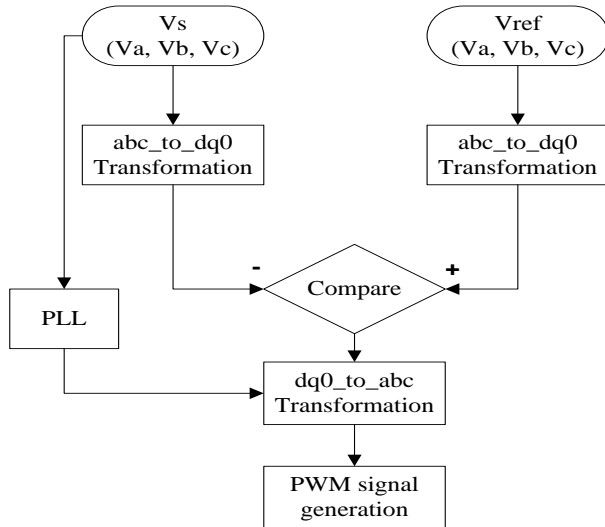


Fig. 4: Block Diagram of Control Technique for DVR Based on Dq0 Transformation.

$$\begin{bmatrix} V_d \\ V_q \\ V_o \end{bmatrix} = \begin{bmatrix} \cos(\theta) & \cos(\theta - \frac{2\pi}{3}) & 1 \\ -\sin(\theta) & -\sin(\theta - \frac{2\pi}{3}) & 1 \\ \frac{1}{2} & \frac{1}{2} & \frac{1}{2} \end{bmatrix} \begin{bmatrix} V_a \\ V_b \\ V_c \end{bmatrix} \quad (6)$$

Equation (6) defines the transformation from three phase system a, b, c to dqo stationary frame. In this transformation, phase A is aligned to the d-axis that is in quadrature with the q-axis. The theta (θ) is defined by the angle between phase A to the d-axis.

2.5. Compensation technique used for DVR

In general, three techniques such as pre-sag, in-phase and in-phase advanced/energy optimization injection techniques are utilized to calculate the injection voltage of DVR [19]. In this paper, in-phase compensation technique which is recommended for linear load is used to calculate the injection voltage of DVR because of its simple implementation and fast response in calculating the compensating voltage. During voltage sag a DVR can compensate the voltage drop across a load by injecting a voltage in-phase with the source voltage through a series connected injection transformer and makes the load voltage magnitude as it was before sag as shown in figure 5. In normal operating condition, the supply voltage (V_{presag}) is equal to the load voltage (V_L) with phase angle zero. During the voltage sag the supply voltage decreases to a value (V_{sag}) less than its nominal value. The DVR responds to the sag event and injects the compensating voltage V_{DVR} in the same phase as the supply voltage to restore the voltage at nominal value.

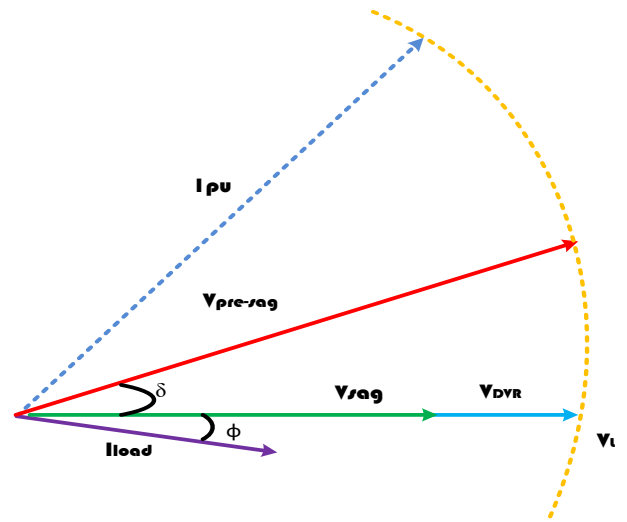


Fig. 5: In Phase Compensation Technique.

The DVR injected voltage (V_{DVR}) can be expressed as:

$$|V_{DVR}| = |V_{presag}| - |V_{sag}| \quad (7)$$

The angle of the injected DVR voltage can be calculated by:

$$\angle V_{DVR} = \theta_{DVR} = 0 \quad (8)$$

θ_{DVR} is the angle of injected DVR voltage (V_{DVR}) with respect to the supply voltage after sag (V_{sag}).

3. Modeling of solar PV generation system

In this section solar PV generation system is described with modeling of solar PV system along with its power conditioning unit (PCU) and control.

3.1. Solar PV system design

The proposed model of solar PV system used in this generation system consists of a solar PV array and PCU for interfacing it to electric utility grid and to local load. A 3- ϕ series RL linear load is considered as local load connected to the solar PV generation system through DVR. The PCU is an electronic device that uses electronic interface, a DC-DC converter with maximum power point tracking (MPPT) capabilities, DC-AC converter (5-level IGBT based VSC) and it is connecting effectively to utility grid. In this manner, solar PV array is capable of independently and simultaneously exchange of active power. Figure 6 shows a schematic block diagram of a solar PV grid connected system, where DC-DC boost converter is controlled to track maximum power points of solar PV arrays using IC MPPT. This converter is connected between solar PV array and DC link capacitors. A pulse width modulation (PWM) controlled IGBT-based 3-level VSC is connected between DC link capacitors C1 and C2 and utility grid through transformer. The AC output of the VSC is connected to grid and the local load through an LC filter which prevents harmonics produced by VSC to penetrate into distribution system. The controlled VSC current compensates reactive current of utility grid depending on load connected and produces active current corresponding to solar PV power output. The parameters which are simulated to control the solar power generation system are maximum power point tracking (MPPT) and voltage control.

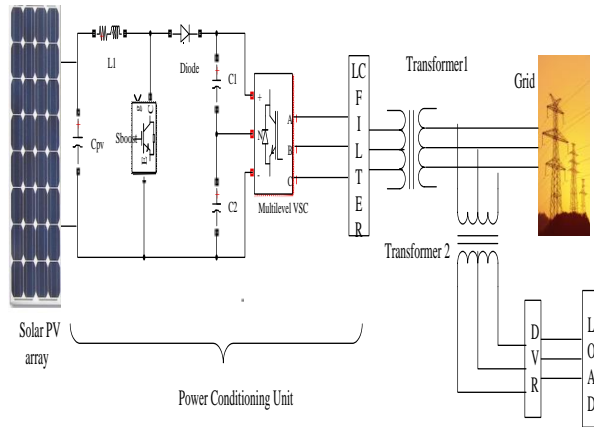


Fig. 6: Block Diagram of a Solar PV Grid Connected System.

3.2. Solar PV cell modelling

Among wide range of renewable energy projects ongoing, the solar PV cell is the most promising future energy technology. The direct conversion of solar radiation into electrical energy by solar PV cells incorporates a number of significant advantages like an electricity generator, along with the significant challenges like energy price, fluctuation of energy, dependence on site and the huge investment requirement. A solar PV array is a combination of both series and parallel solar PV cells. Figure 7 gives the modeling of solar cell with two diode model [20-21], equation (9) governs the characteristics of a solar PV cell which behaves more like a current source and figure 8 gives solar cell I-V and P-V characteristics corresponding to the equation (9).

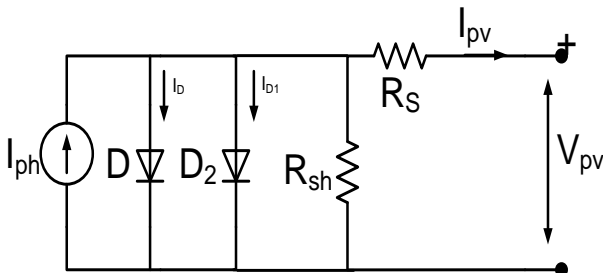


Fig. 7: Electrical Equivalent Circuit of a Solar PV Cell.

$$I_{pv} = I_{ph} - I_s \left[\exp\left\{ \frac{V_{pv} + I_{pv} R_s}{N_1 V_T} \right\} - 1 \right] - I_{s2} \left[\exp\left\{ \frac{V_{pv} + I_{pv} R_s}{N_2 V_T} \right\} - 1 \right] - \frac{V_{pv} + I_{pv} R_s}{R_{sh}} \tag{9}$$

Where:

- I_{pv} Cell output current A
- I_{ph} Photon generated current
- I_s First diode saturation current
- I_{s2} Second diode saturation current
- R_s Series resistance of cell
- R_{sh} Shunt resistance of cell
- V_{pv} Cell's output voltage
- V_T Thermal voltage
- P_M Maximum power obtain from solar PV
- V_M Output voltage of PV array corresponding to maximum power
- I_M Output current of PV array corresponding to maximum power
- N Diode emission coefficient or quality factor of the first diode D
- $N2$ Diode emission coefficient or quality factor of the second diode D2

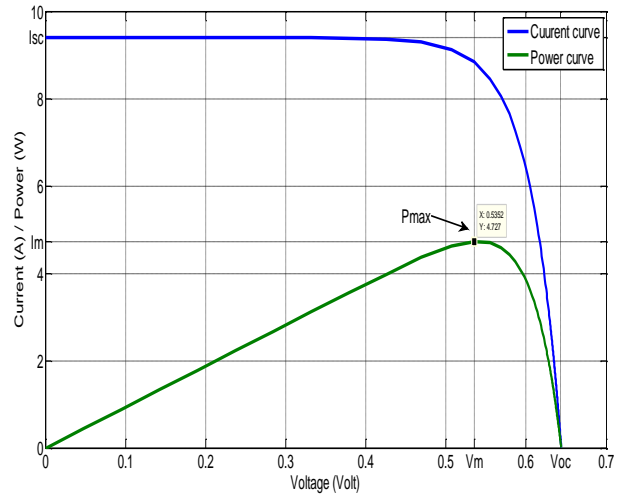


Fig. 8: Solar Cell I-V and P-V Characteristics.

3.3. Control of solar PV generation system

In this paper, a solar PV generation system considered and it delivers power to the grid and to the local load. The characteristics of solar PV are significantly influenced by parameters like insolation, temperature and partial shading. Any change in environment conditions would alter the output power of the PV array [22]. To track the maximum power with these environmental issues solar PV system needs an electronic circuitry which is called maximum power point tracker (MPPT). By associating the MPPT in the solar PV system, it is possible to always ensure the maximum output power under the corresponding environment conditions. There are various MPPT algorithms proposed in the research publications [23-24]. In this paper, the incremental conductance (IC) method is used to match the characteristics of module with respect to maximum power to avoid the power loss. MPPT algorithms are essential because PV arrays exhibit nonlinear voltage-current characteristics with a unique point at which maximum power is produced.

3.4. Boost converter modelling

Boost converter also called voltage step up converter is employed in PCU to get higher output voltage (V_o) from lower input voltage (V_i). The boost converter topology is shown in figure 9. In case of MPPT operation boost converter is used to match the impedance of source or solar array to obtain maximum power.

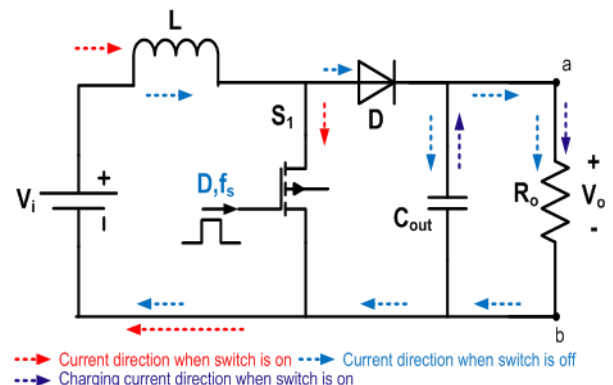


Fig. 9: Boost Converter Topology

The operating principle of boost converter is describe as, when the switch S_1 is turned on by the pulse of PWM generator, current flows through inductor (L) and energy is stored in the form of magnetic field and induces a voltage across it. When switch is turned off, induced voltage across the inductor, (L) adds to the input voltage. The voltage across the inductor and input voltage are in series and collectively these two charges the output capacitor (C_{out}) to a voltage more than input voltage. While designing the boost converter [25],

the duty cycle for required output voltage is calculated by equation (10)

$$D = 1 - \frac{V_i}{V_o} \tag{10}$$

Selection of inductor: The value of inductor is chosen on the basis of estimated ripple current of inductor at maximum input voltage, given by equation (11).

$$L = \frac{V_i \times (V_o - V_i)}{\Delta I_L \times f_s \times V_o} \tag{11}$$

Where $\Delta I_L = 0.1 I_L$ is the estimated inductor ripple current. For continuous conduction mode the minimum inductance required is LC and calculated as:

$$L_C = \frac{D \times (1-D)^2 R_o}{2f_s} \tag{12}$$

Selection of capacitor: The value of capacitor is calculated by the change in output voltage or ripple given in equation (13):

$$C = \frac{D}{R_o \times f_s \times (\Delta V_o / V_o)} \tag{13}$$

Where ΔV_o is desired output voltage ripple, for 0.01 voltage ripple corresponding to output voltage equation (13) becomes:

$$C = \frac{D}{R_o \times f_s \times 0.01} \tag{14}$$

3.5. Maximum power point technique used for solar PV system

There are many MPPT algorithms reported in literature. The comparison among different maximum power point tracking techniques is presented in ref. [23-24]. The main techniques have been found to be perturb & observe, IC, constant voltage, fuzzy logic control, data-based look up table, neural network, and ripple correlation factor etc. However, we have implemented incremental conductance (IC) technique [26-28] which can efficiently track maximum power of solar PV system even under changing weather conditions. The IC technique is a simple approach which actually matches the incremental conductance to the instantaneous conductance and at the time of MPP both becomes equal. This method is based on the fact that slop of the PV array power curve is zero at the MPP (Pmax) as shown in figure 8.

This can be expressed as follows:

Power: $P = V \times I$

$$\frac{dP}{dV} = I + V \frac{dI}{dV}$$

At true MPPT

$$\frac{dP}{dV} = 0$$

$$I + V \frac{dI}{dV} = 0$$

$$\frac{dI}{dV} = -\frac{I}{V} \tag{15}$$

Where dI/dV : Incremental conductance,
 I/V : Instantaneous conductance.

Equation (15) shows that MPP can be evaluated by comparing instantaneous conductance to the incremental conductance. The operation of this technique can be divided in three regions as shown in Table 1.

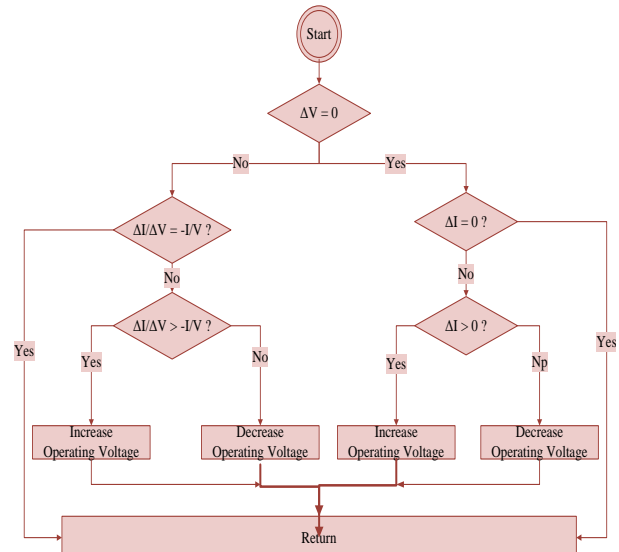


Fig. 10: Flow Chart of Incremental Conductance MPPT.

The flow chart of the method is given in Figure 10. The method is complex and computationally more demanding as compared to P&O [29].

4. Proposed system

In the proposed system given in this paper a solar PV generation system of 99 kW is considered with IC MPPT with a DC link of voltage 500 V feeding to grid through VSC. The DVR is connected in between solar PV system and load that also uses the photovoltaic (PV) system as alternative DC source as shown in Figure 11. The DC-DC boost converter (5 kHz) produces a chopped output voltage, and thus controls average DC voltage relation between its output and input aiming at continuously matching characteristics of solar PV system to equivalent impedance presented by DC bus of IGBT based VSC. DC-DC converter duty ratio is initially set at 0.5. The incremental conductance (IC) maximum power point tracking (MPPT) method is employed for the boost converter in PCU of solar photovoltaic (PV) based generation system, and at the same instance, proportional integral (PI) controller is used to control the DVR output voltage during the fault. As demonstrated in figure 11, a DVR section is comprised of a NPC multilevel inverter along with solar PV as an active power generator. The aim of this control is to regulate and maintain load voltage magnitude constant at point where a sensitive linear load is connected during voltage disturbances. To control the switching pulses for NPC, PI controller is used. Modeling of solar PV array is done by adopting following parameters shown in Table 2.

Table 1: Methodology of IC Method

S. No.	MPP position	Power and Voltage relation
1	Before MPP	$\frac{dP}{dV} > 0$ or $\frac{dI}{dV} + \frac{I}{V} > 0$
2	After MPP	$\frac{dP}{dV} < 0$ or $\frac{dI}{dV} + \frac{I}{V} < 0$
3	At MPP	$\frac{dP}{dV} = 0$ or $\frac{dI}{dV} + \frac{I}{V} = 0$

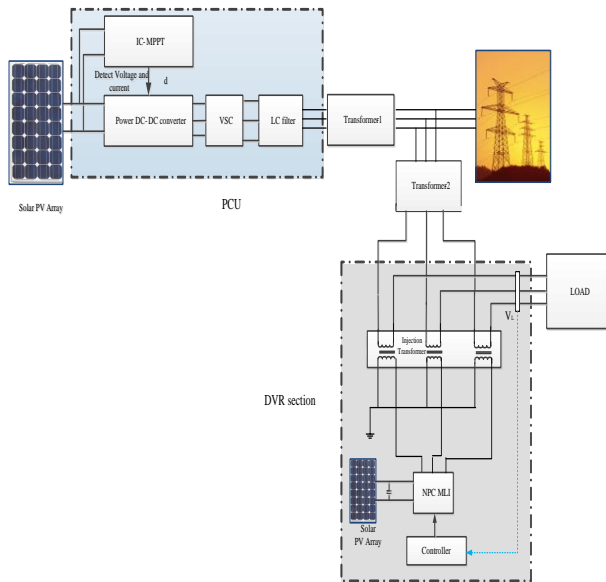


Fig. 11: Block Diagram of Solar PV Fed Grid System with DVR.

Table 2: Specifications Adopted for Solar PV Array

S.No.	System Parameter	Rating/Values
1	No. of parallel string	66
2	No. of series connected modules per string	5
3	Module specification under STC [V _{pv} , I _{pv} , V _M , I _M]	81V, 6.85A, 60V, 5A
4	Model parameter for module [R _{sh} , R _s , I _s , I _{ph} , N]	49.5556Ω, 2.2134Ω, 1.938e-10A, 6.7045A, 3.6458
5	Maximum power of array P _{Max}	99 kW
6	Irradiation and temperature	1000w/m2 and 250C

Parameters used for modeling of DVR are presented in Table 3.

Table 3: Specifications Adopted for DVR Modeling

S. No.	System Parameter	Rating/Values
1)	Nominal DC voltage of solar array	300V
2)	Nominal power and frequency	30kW and 50Hz
3)	PI controller [K _p , K _i]	0.5, 50
4)	Sample time	50×10 ⁻⁶ s
5)	LC filter [L, C]	2mH, 15μF

5. Simulation of control schemes and results

To prove capabilities of above mentioned control schemes, the solar PV grid connected test system with IC MPPT and DVR with PI controller is modeled with Matlab/Simulink.

5.1. Solar PV grid connected system without fault

Figure 12 and 13 shows the I-V and P-V characteristics of Xunlight XR36-300 array with different temperature and different insolation respectively. Figure 14 depicts the active and reactive power waveform of solar PV array. Active power is supplied by the PV system to grid, and no reactive power flow takes place in this system. The voltage output of the solar PV system is 300V dc which supplied to the boost converter which is operated with 5 kHz switching frequency, here output of boost converter is 500V dc and it is shown in figure 15. The output of boost converter is controlled by IC MPPT technique. The output of this boost converter is given to the VSC, VSC is controlled by PI (voltage regulator gain $k_p=7$, $k_i=800$ and current regulator gain $k_p=0.3$, $k_i=20$) controller, which gives ac output voltage and current as shown in figure 16 (a) and (b) respectively. The output voltage of VSC is 260V stepped up into 11kV (rms L-L) using transformer than fed to grid. The grid voltage and current is shown in figure 17 (a) and (b) respectively.

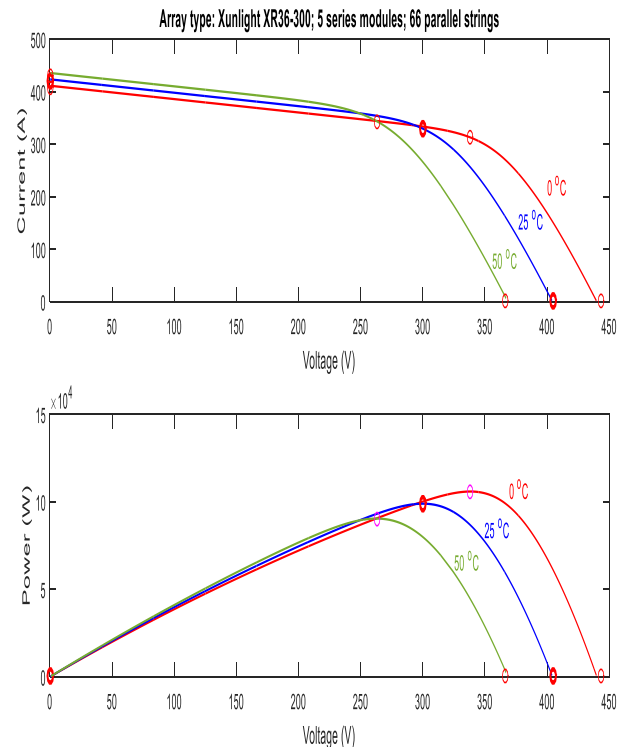


Fig. 12: I-V and P-V Characteristic with Different Temperature.

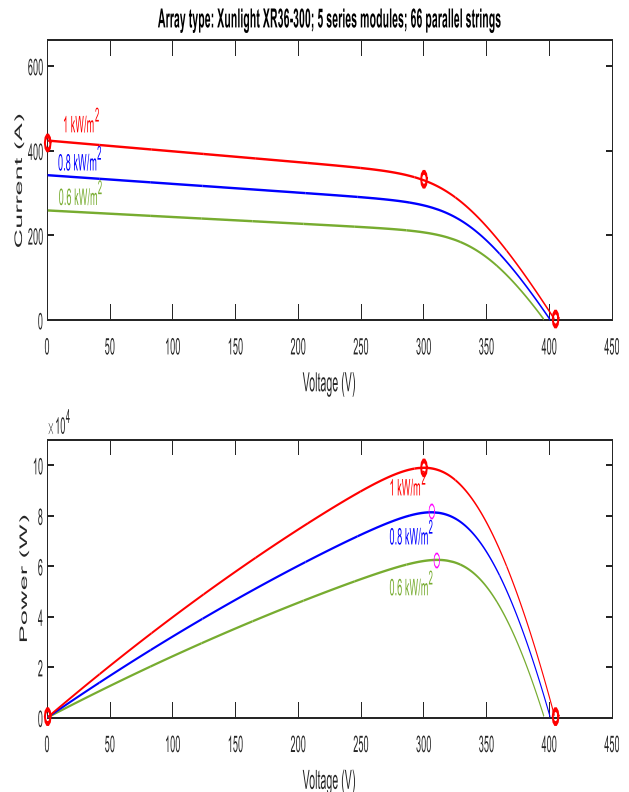


Fig. 13: I-V and P-V Characteristic with Different Insolation.

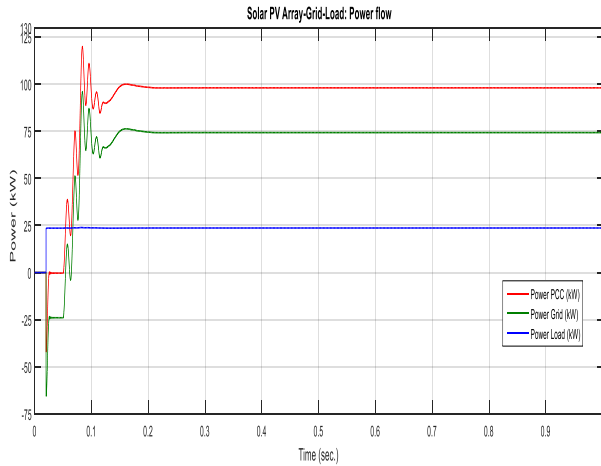


Fig. 14: Active Power from Solar PV Array to Grid and Load with MPPT Control.

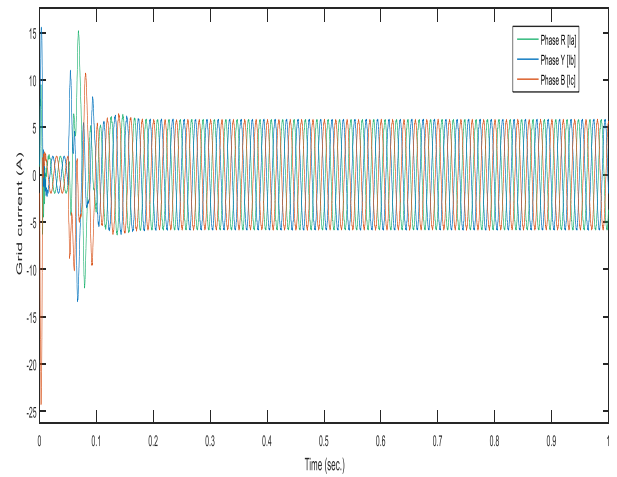


Fig. 17: With MPPT Control Grid Current.

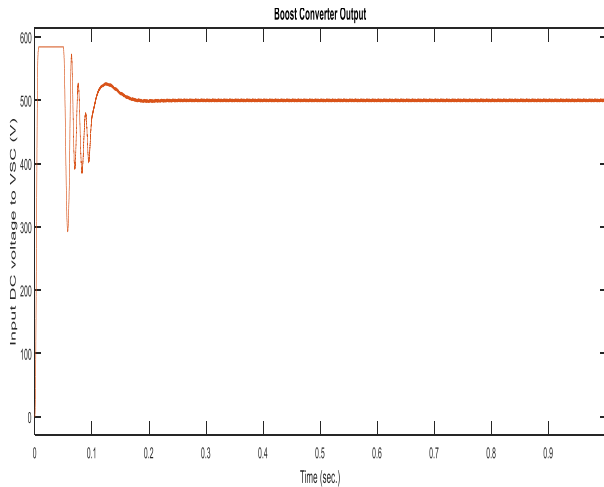


Fig. 15: Boost Converter Output Voltage or DC Link Voltage.

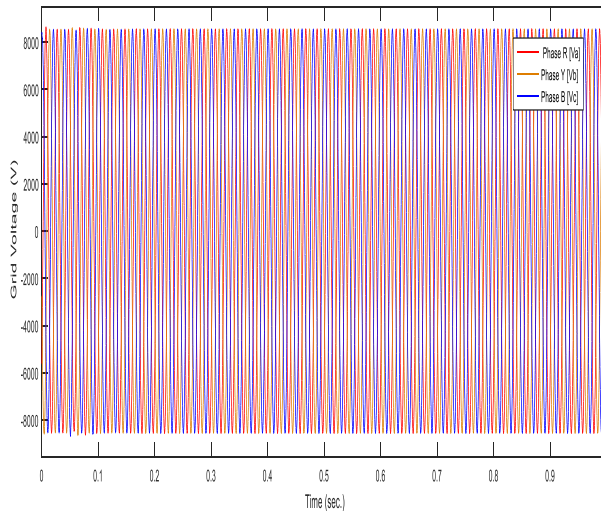


Fig. 16: With MPPT Control Grid Voltage.

5.2. Effect of 3- ϕ fault on load

The load is connected parallel to the grid; the grid voltage is stepped down into 440V and supplied to the RL load. In between solar PV system and load a DVR is connected in series which is also fed by solar PV array of 300V, here solar is used as an alternative DC source. When the 3- ϕ fault occurs in the line parallel to the grid, during the time 0.5s to 0.7s the output voltage across the load experiences a sag of 65% wrt to rated, and at the same time current is also decrease as shown in the figure 18 (a) and (b) respectively. To mitigate the sag DVR will operate during 0.5s to 0.7s and compensate for the sag and restore 96.79% of the pre sag voltage magnitude and current as shown in the figure 19 (a) and (b) with the 7.17 % THD and 7.20 % THD respectively shown in figure 20 (a) and (b).

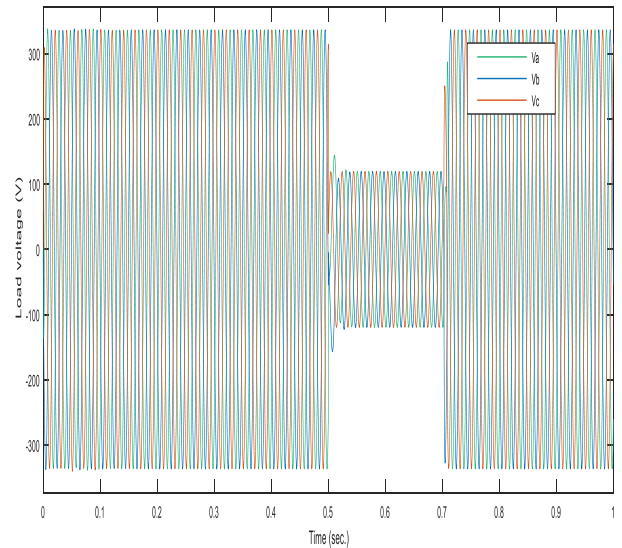


Fig. 18: (A) Load Voltage without DVR with Fault.

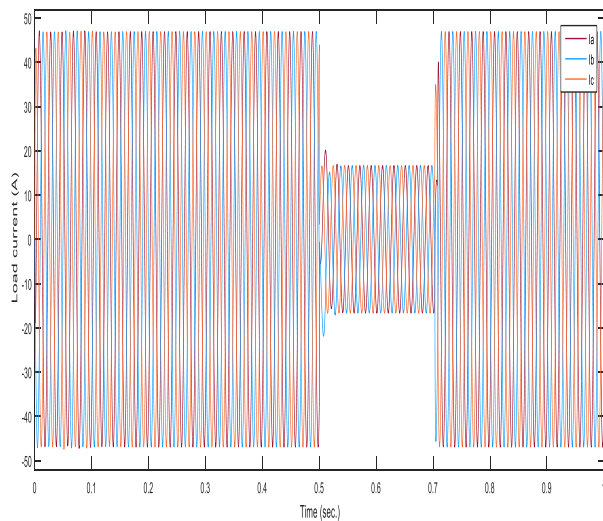


Fig. 18: (B) Load Current without DVR with Fault.

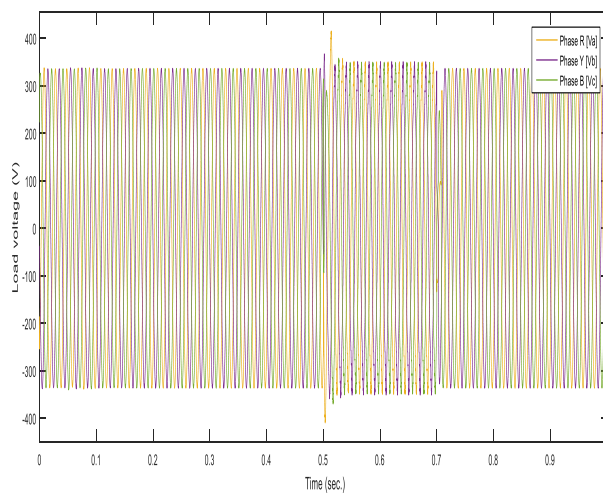


Fig. 19: (A) Load Voltage with DVR.

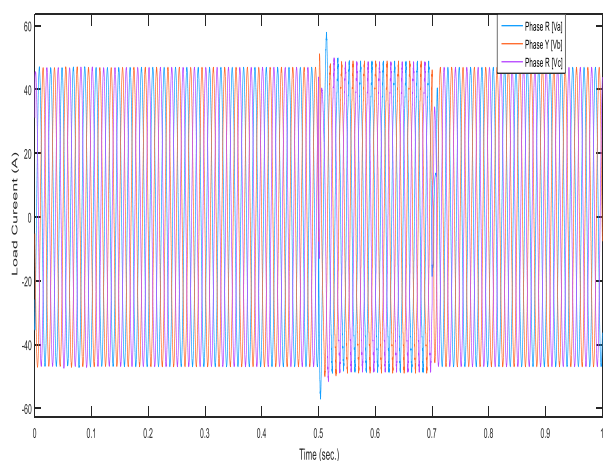


Fig. 19: (B) Load Current with DVR.

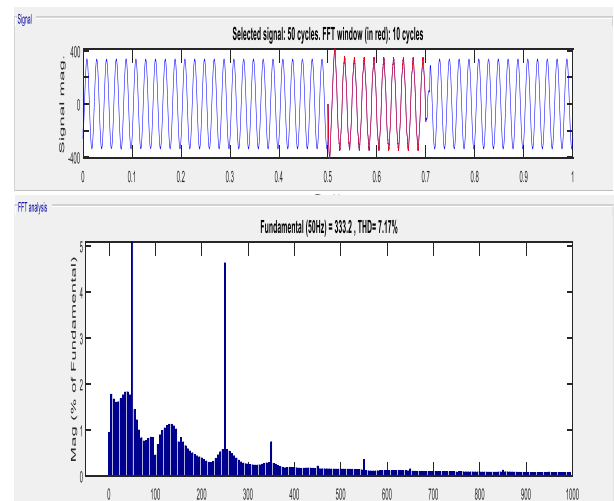


Fig. 20: (A) Load Voltage Percentage THD with DVR.

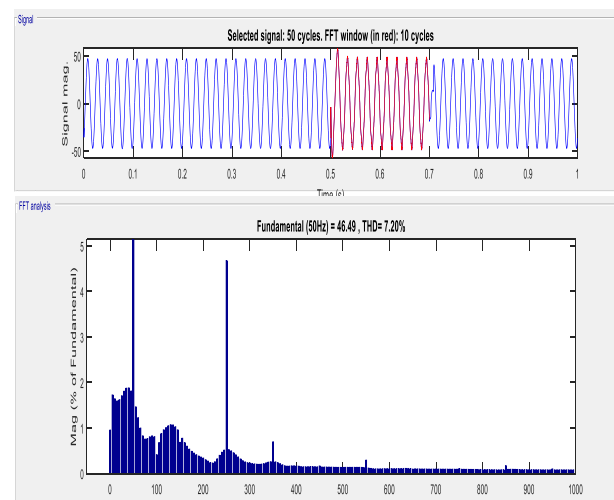


Fig. 20: (B) Load Current Percentage THD with DVR.

6. Conclusion

This paper has accentuated an approach of modeling and simulation for a three-phase grid connected 99 kW solar PV system with related control strategies. MPPT operation is performed by means of boost converter and control signal generated through IC method of MPPT. Three-phase five-level VSC is used to convert boosted voltage into AC to supply grid. A PI controlled DVR is also realized in which investigations of THD is carried out during faulted conditions. IC method is fast as compared to the P&O method as well as it purges the steady state oscillations at the point of maximum power. From the simulation results it is marked that active power transfer takes place with accurate tracking of maximum power. Primarily whole active power is being supplied to grid before the occurrence of fault. During the fault DVR compensate the voltage sag and the proposed multilevel inverter based DVR compensate sag and restore 96.79% of the pre sag voltage magnitude and current with the 7.17% THD and 7.20 % THD respectively.

References

- [1] Cambell A. and McHattie R., (1999) "Backfilling the sinewave. A dynamic voltage restorer case study," *Power Engineering Journal*, vol. 13, no. 3, pp. 153 – 158. <https://doi.org/10.1049/pe:19990309>.
- [2] Benachaiba C. and Ferdi B., (2009) "Power quality improvement using DVR," *American Journal of Applied Sciences*, vol. 6, no. 3, pp. 396-400. <https://doi.org/10.3844/ajassp.2009.396.400>.
- [3] Omar R. and Sulaiman M., (2011) "Dynamic voltage restorer application for power quality improvement in electrical distribution system: An overview," *Australian Journal of Basic and Applied Sciences*, vol. 5, no. 12, pp. 379-396.

- [4] Wijekoon H.M., Vilathgamuwa D.M. and Choi, S.S., (2003) "Inter-line dynamic voltage restorer: an economical way to improve inter-line power quality," *Generation, Transmission and Distribution, IEE Proceedings*, vol. 150, no. 5, pp. 513-520. <https://doi.org/10.1049/ip-gtd:20030800>.
- [5] Sadigh A. K. and Smedley K. M., (2012) "Review of voltage compensation methods in dynamic voltage restorer (DVR)," *IEEE Power and Energy Society General Meeting 2012*, pp. 1-8. <https://doi.org/10.1109/PESGM.2012.6345153>.
- [6] Ramachandaramurthy V. K., Fitzer C., Arulampalam A., Zhan C., Barnes M., and Jenkins, N., (2002) "Control of a battery supported dynamic voltage restorer," *IEE Proceedings-Generation, Transmission and Distribution*, vol. 149, no. 5, pp. 533-542. <https://doi.org/10.1049/ip-gtd:20020658>.
- [7] Omar R and Rahim NA., (2012) "Voltage unbalanced compensation using dynamic voltage restorer based on super capacitor," *International Journal of Electrical Power & Energy System*, vol. 43, no. 1, pp. 573-81. <https://doi.org/10.1016/j.ijepes.2012.05.015>.
- [8] Sundarabalan C. K. and K. Selvi, (2015) "Compensation of voltage disturbances using PEMFC supported dynamic voltage restorer," *International Journal of Electrical Power & Energy Systems*, vol. 71, pp. 77-92. <https://doi.org/10.1016/j.ijepes.2015.02.032>.
- [9] Ramasamy M. and Thangavel S., (2012) "Photovoltaic based dynamic voltage restorer with power saver capability using PI controller," *International Journal of Electrical Power & Energy Systems*, vol. 36, no. 1, pp. 51-59. <https://doi.org/10.1016/j.ijepes.2011.10.023>.
- [10] Ramasamy M. and Thangavel S., (2013) "Experimental verification of PV based dynamic voltage restorer (PV-DVR) with significant energy conservation," *International Journal of Electrical Power & Energy Systems*, vol. 49, pp. 296-307. <https://doi.org/10.1016/j.ijepes.2013.01.018>.
- [11] Chankhamrian W., Winittham C., Bhumkittipich K. and Manmai, S., (2014) "Load-side voltage compensation of small hydropower grid-connected system using DVR based on PV source," *Energy Procedia*, vol. 56, pp. 610-620. <https://doi.org/10.1016/j.egypro.2014.07.200>.
- [12] Gupta A., Chanana S. and Thakur, T. (2015) "Power quality assessment of a solar photovoltaic two-stage grid connected system: Using fuzzy and proportional integral controlled dynamic voltage restorer approach," *Journal of Renewable and Sustainable Energy*, vol. 7, no. 1, pp. 1-18. <https://doi.org/10.1063/1.4906980>.
- [13] Srisailam C. H. and Sreenivas A., (2012) "Mitigation of voltage sags/swells by dynamic voltage restorer using PI and fuzzy logic controller," *International Journal of Engineering Research and Applications*, vol. 2, no. 4, pp.1733-1737.
- [14] Anaya-Lara O. and E. Acha, (2002) "Modeling and analysis of custom power systems by PSCAD/EMTDC," *IEEE Transactions on Power Delivery*, vol. 17, no.1, pp. 266-272. <https://doi.org/10.1109/61.974217>.
- [15] Salimin R. H. and Rahim M. S. A., (2011) "Simulation analysis of DVR performance for Voltage sag mitigation," In *5th International Power Engineering and Optimization Conference (PEOCO)*, IEEE pp. 261-266.
- [16] Meyer, C., Romaus, C. and De Doncker, R.W., (2005) "Five level neutral-point clamped inverter for a dynamic voltage restorer" In *Power Electronics and Applications, 2005 IEEE European Conference on*, pp. 9-pp.
- [17] Tran, H.N., Dzung, P.Q., Le, N.A. and Nguyen, T.D., (2016) "Dynamic voltage restorer-multilevel inverter based on predictive voltage controller" In *IEEE International Conference on Sustainable Energy Technologies (ICSET)*, pp. 174-179. <https://doi.org/10.1109/ICSET.2016.7811777>.
- [18] Babaei E., Kangarlu M. F. and Sabahi M., (2014) "Dynamic voltage restorer based on multilevel inverter with adjustable dc-link voltage," *IET Power Electronics*, vol. 7, no. 3, pp. 576-590. <https://doi.org/10.1049/iet-pel.2013.0179>.
- [19] Jayaprakash P., Singh B., Kothari D. P., Chandra A. and Al-Haddad K., (2014) "Control of reduced-rating dynamic voltage restorer with a battery energy storage system," *IEEE Transactions on Industry Applications*, vol. 50, no. 2, pp. 1295-1303. <https://doi.org/10.1109/TIA.2013.2272669>.
- [20] Nema S., Nema R. K. and Agnihotri G., (2010) "MATLAB/Simulink based study of photovoltaic cells/modules/array and their experimental verification," *International journal of Energy and Environment*, vol. 1, no. 3, pp. 487-500, 2010.
- [21] Rahman S. A., Varma R. and Vanderheide T., (2014) "Generalised model of a photovoltaic panel," *IET Renewable Power Generation*, vol. 8, no. 3, pp. 217-229. <https://doi.org/10.1049/iet-rpg.2013.0094>.
- [22] Verma D., Nema S., Shandilya A.M. and Dash S.K., (2015) "MATLAB (Simscape) simulation and experimental validation of solar photovoltaic system for performance analysis under varying environmental and mismatch condition," *Electrical and Electronics Engineering: An International Journal (ELELIJ)*, vol. 4, no. 3, pp. 39-54. <https://doi.org/10.14810/elej.2015.4304>.
- [23] Verma D., Nema S., Shandilya A.M. and Dash S.K., (2016) "Maximum power point tracking (MPPT) techniques: Recapitulation in solar photovoltaic systems," *Renewable and Sustainable Energy Reviews*, vol. 54, pp.1018-1034. <https://doi.org/10.1016/j.rser.2015.10.068>.
- [24] Verma D., Nema S., Shandilya A.M. and Dash S.K., (2015) "Comprehensive analysis of maximum power point tracking techniques in solar photovoltaic systems under uniform insolation and partial shaded condition," *Journal of Renewable and Sustainable Energy*, vol. 7, no. 4, pp.042701. <https://doi.org/10.1063/1.4926844>.
- [25] Verma D., Nema S. and Shandilya A.M., (2016) "A different approach to design non-isolated DC-DC converters for maximum power point tracking (MPPT) in solar photovoltaic systems," *Journal of Circuits, Systems, and Computers: World Scientific Publication*, vol. 25, no. 8, pp. 1630004. <https://doi.org/10.1142/S021812661630004X>.
- [26] Kish G. J., Lee J. J., and Lehn, P., (2012) "Modeling and control of photovoltaic panels utilising the incremental conductance method for maximum power point tracking," *IET Renewable Power Generation*, vol. 6, no. 4, pp. 259-266. <https://doi.org/10.1049/iet-rpg.2011.0052>.
- [27] Liu F., Duan S., Liu F., Liu B., and Kang, Y., (2008) "A variable step size INC MPPT method for PV systems," *IEEE Transactions on Industrial Electronics*, vol. 55, no. 7, pp. 2622-2628. <https://doi.org/10.1109/TIE.2008.920550>.
- [28] Kjaer and Soren B, (2012) "Evaluation of the hill climbing and the incremental conductance maximum power point trackers for photovoltaic power systems," *IEEE Transactions on Energy Conversion*, vol. 27, no. 4, pp. 922-929. <https://doi.org/10.1109/TEC.2012.2218816>.
- [29] Dash S. K., Verma D., Nema S. and Nema R. K., (2014) "Comparative analysis of maximum power point (MPP) tracking techniques for solar PV application using MATLAB simulink," In *Recent Advances and Innovations in Engineering (ICRAIE)*, IEEE, pp. 1-7.